

Red laser induced upconversion luminescence in Er-doped calcium aluminum germanate garnet

Xiao Zhang, Jianhui Yuan, Xingren Liu, Jean Pierre Jouart, and Gérard Mary

Citation: *J. Appl. Phys.* **82**, 3987 (1997); doi: 10.1063/1.365707

View online: <http://dx.doi.org/10.1063/1.365707>

View Table of Contents: <http://jap.aip.org/resource/1/JAPIAU/v82/i8>

Published by the [American Institute of Physics](#).

Related Articles

Tunability of terahertz random lasers with temperature based on superconducting materials
J. Appl. Phys. **112**, 043111 (2012)

Film thickness and grating depth variation in organic second-order distributed feedback lasers
J. Appl. Phys. **112**, 043104 (2012)

Development of a YAG laser system for the edge Thomson scattering system in ITER
Rev. Sci. Instrum. **83**, 10E344 (2012)

Low threshold amplified spontaneous emission from dye-doped DNA biopolymer
J. Appl. Phys. **111**, 113107 (2012)

Electrically pumped wavelength-tunable blue random lasing from CdZnO films on silicon
Appl. Phys. Lett. **100**, 231101 (2012)

Additional information on J. Appl. Phys.

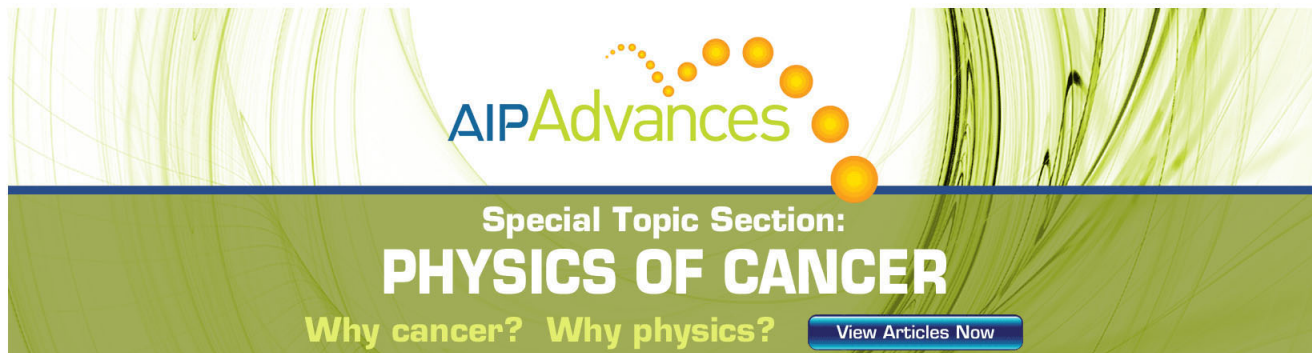
Journal Homepage: <http://jap.aip.org/>

Journal Information: http://jap.aip.org/about/about_the_journal

Top downloads: http://jap.aip.org/features/most_downloaded

Information for Authors: <http://jap.aip.org/authors>

ADVERTISEMENT



AIP Advances

Special Topic Section:
PHYSICS OF CANCER

Why cancer? Why physics? [View Articles Now](#)

Red laser induced upconversion luminescence in Er-doped calcium aluminum germanate garnet

Xiao Zhang, Jianhui Yuan, and Xingren Liu^{a)}

Changchun Institute of Physics, Chinese Academy of Sciences, 130021 Changchun, People's Republic of China

Jean Pierre Jouart and Gérard Mary

Laboratoire d'Energétique et d'Optique, UTAP, Université de Reims, B.P. 1039, 51687 Reims cedex, France

(Received 2 April 1997; accepted for publication 2 July 1997)

In this work, we have studied the spectroscopic and dynamic properties of the green (${}^4S_{3/2} \rightarrow {}^4I_{15/2}$) and blue (${}^2P_{3/2} \rightarrow {}^4I_{11/2}$) upconversions for a series of Er³⁺ doped Ca₃Al₂Ge₃O₁₂, induced by a red tunable laser excitation. The green emission is due to either an energy transfer involving two ions excited in the ${}^4I_{11/2}$ multiplet or an excited state absorption from the ${}^4I_{13/2}$ level, depending on whether the laser excitation wavelength is tuned on ${}^4I_{15/2} \rightarrow {}^4F_{9/2}$ or ${}^4I_{13/2} \rightarrow {}^4F_{5/2}$. The blue emission mainly results from a three-step absorption process through the ${}^4I_{13/2}$ and ${}^4S_{3/2}$ multiplets. The temperature and concentration effects have been analyzed for the green and blue upconversions.

© 1997 American Institute of Physics. [S0021-8979(97)00720-2]

I. INTRODUCTION

Upconversion luminescence is a well-known phenomenon in rare earth doped crystalline and glass materials. The successive absorption, the energy transfer, the cooperative process, and the photon avalanche effect are the principal upconversion processes identified.¹⁻⁸ Frequency upconversion has been recognized as early as the 1950's,³ which induced research for infrared quantum counts later in the 60's, and there has been renewed interest recently owing to the great achievement of high power III-V semiconductor laser diodes potentially enabling infrared pumped, compact upconversion lasers.

So far, upconversion fluorescence have been observed for many trivalent rare earth ions such as Er³⁺, Tm³⁺, Ho³⁺, Nd³⁺, Pr³⁺, and Eu³⁺ in various materials and, in particular, in fluoride crystals and glasses. Among the rare earth ions, Er³⁺ is the most popular as well as one of the most efficient ions in this respect, and Er³⁺ upconversion laser operation has been achieved both at 77 K and at room temperature.⁹ Compared with the fluoride system, the upconversion process is seldom observed in oxide crystals and glasses without cooling the sample to low temperature, because of the higher vibration energy in oxides. On the other hand, the oxide materials have advantageous application properties compared to fluorides such as higher chemical durability and thermal stability. Recently, several upconversion studies have been realized in heavy metal oxide glass systems and garnets.¹⁰⁻¹² They have shown efficient upconversion even at room temperature.

In a recent paper,¹³ we have briefly reported the excited state absorption and efficient upconversion in Er-doped calcium aluminum germanate garnet (CAGG) polycrystalline material. In this article, a systematic investigation has been applied for this system by analyzing temperature effects,

concentration effects, and the dynamic properties for the green and blue upconversions. The upconversion spectra were recorded in several spectral ranges resulting from three energy levels: ${}^4S_{3/2}$, ${}^2P_{3/2}$, and ${}^2H_{11/2}$. The luminescence intensity is comparable with that in the fluorite crystals even at room temperature. Three-photon upconversion has been observed for the emissions originating from the ${}^2P_{3/2}$ level.

II. EXPERIMENT

The samples used in this work were synthesized by high temperature solid state reactions. The starting materials are high purity CaO, Al₂O₃, and GeO₂, which are mixed with the stoichiometric ratio as Ca_{3-x}Er_xAl₂Ge₃O₁₂, where x varies from 0.005 to 0.1. The Er³⁺ was introduced as Er₂O₃ with the 5N purity. The well mixed batches were introduced into a furnace, and were gradually fired at 900, 1000, and 1250 °C for 4 h. After each firing, the products were ground into fine powder. The final samples were checked by x-ray diffraction, and the cubic garnet structure was obtained.

The upconversion study was performed at room temperature and at 100 K. A cw Ar⁺ laser (Spectra Physics 2000) pumped tunable dye laser (Spectra Physics 375) was used as the excitation source. Kiton red dye was used to supply red laser emission between 620 and 670 nm (16 200–15 000 cm⁻¹). Powder samples were mixed with gel, coated to a glass support, and fixed in a cryostat cooled by liquid nitrogen to about 100 K. The excitation light was introduced at a 45° angle, and the luminescence signal was reflected to the entrance of a Coderg T800 three grating monochromator. The emission from the sample was detected by a water-cooled photomultiplier (EMI 9558 QB). The luminescence decay and rise times were measured with a Metrix Oscillograph (OX 750-2). The laser beam was modulated by a Pockels cell, and the rise and decay signals were analyzed by a microcomputer.

III. EXPERIMENTAL RESULTS AND DISCUSSION

The upconversion emission spectra for the CAGG:1% Ho³⁺ induced by red laser excitation are shown in Fig. 1.

^{a)}Also with: Laboratory of Excited State Processes, Chinese Academy of Sciences, 130021 Changchun, People's Republic of China.

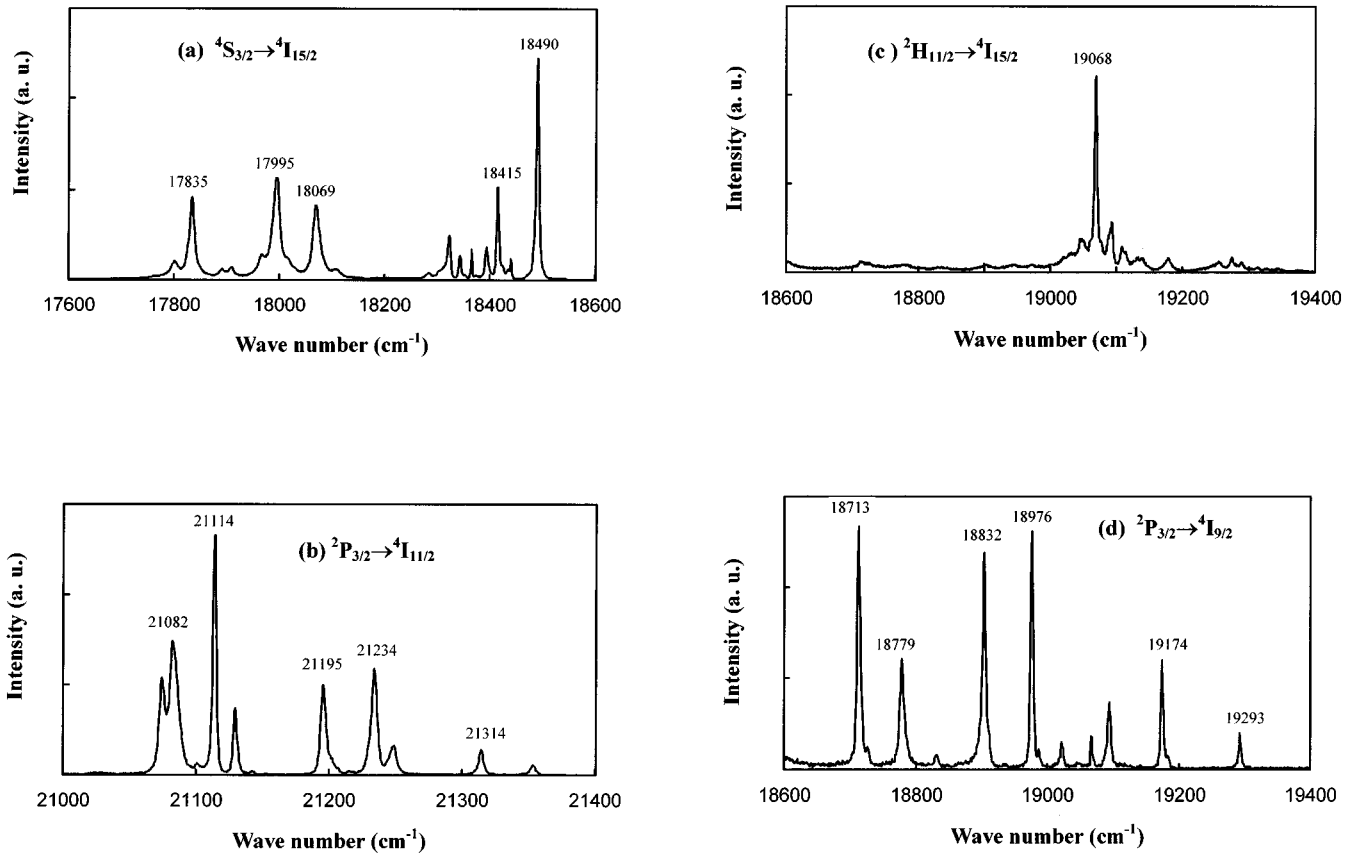


FIG. 1. Upconversion spectra obtained from three energy levels: ${}^4S_{3/2}$, ${}^2P_{3/2}$, and ${}^2H_{11/2}$ for CAGG:1% Er^{3+} : (a) ${}^4S_{3/2} \rightarrow {}^4I_{15/2}$, (b) ${}^2P_{3/2} \rightarrow {}^4I_{11/2}$, (d) ${}^2P_{3/2} \rightarrow {}^4I_{9/2}$ at 100 K and (c) ${}^2H_{11/2} \rightarrow {}^4I_{15/2}$ at 300 K.

These spectra are mainly located at three spectral ranges, as depicted in Figs. 1(a)–1(d). According to the energy level diagram of the Er^{3+} , these spectra can be ascribed to the transitions: ${}^4S_{3/2} \rightarrow {}^4I_{15/2}$, ${}^2P_{3/2} \rightarrow {}^4I_{11/2}$, ${}^2H_{11/2} \rightarrow {}^4I_{15/2}$, and ${}^2P_{3/2} \rightarrow {}^4I_{9/2}$, respectively. Three other weak upconversion emissions have been detected in the red and infrared ranges

due to the transitions: ${}^2P_{3/2} \rightarrow {}^4F_{9/2}$, ${}^2P_{3/2} \rightarrow {}^4S_{3/2}$, and ${}^2H_{11/2} \rightarrow {}^4I_{13/2}$. The most intense upconversion is observed at the green region due to the ${}^4S_{3/2} \rightarrow {}^4I_{15/2}$ transition, which is even more intense than the red Stokes emission ${}^4F_{9/2} \rightarrow {}^4I_{15/2}$.

The excitation spectra for the red Stokes emission, green and blue upconversions differ one from another, and these spectra are given in Fig. 2. For the red emission, almost all the excitation peaks arise from the ground state absorption (GSA), viz. ${}^4I_{15/2} \rightarrow {}^4F_{9/2}$, ranging from 15 200 to 15 600 cm^{-1} . For the green emission, in addition to the GSA lines, another group of excitation peaks has been observed in the higher energetic side between 15 500 and 15 800 cm^{-1} .

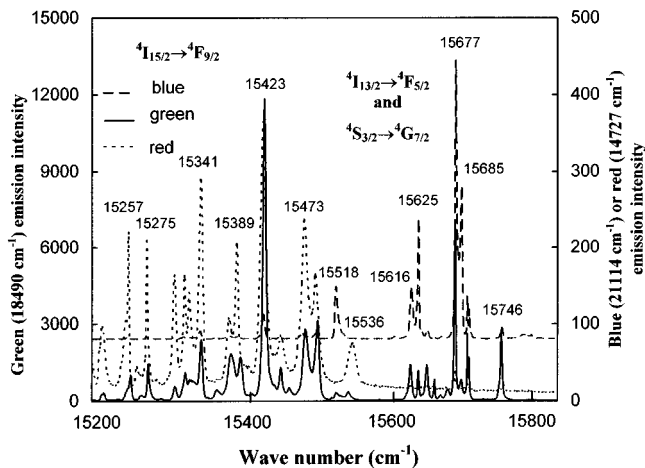


FIG. 2. Excitation spectra (recorded at 100 K) for green, blue and red emissions of CAGG:1% Er^{3+} . These spectra were obtained by monitoring the 18 490 cm^{-1} green (—), 14 729 cm^{-1} red (---), and 21 114 cm^{-1} blue (---) emissions excited with red dye laser. (The profile for green emission is shifted upward referring to the others).

TABLE I. Positions of the Stark sublevels of Er^{3+} in CAGG.

Level	Energy (cm^{-1})
${}^4I_{15/2}$	0, 50, 93, 131, 147, 420, 524, 580
${}^4I_{13/2}$	6614, 6667, 6675, 6693, 6776, 6831, 6919
${}^4I_{11/2}$	10 264, 10 303, 10 369, 10 384, 10 416, 10 423
${}^4I_{9/2}$	12 324, 12 522, 12 594, 12 719, 12 785
${}^4F_{9/2}$	15 307, 15 319, 15 325, 15 473, 15 536
${}^4S_{3/2}$	18 415, 18 490
${}^2H_{11/2}$	19 110, 19 116, 19 132, 19 142, 19 182
${}^4F_{5/2}$	22 291, 22 312, 22 360
${}^2P_{3/2}$	31 498, 31 617
${}^4G_{7/2}$	34 092, 34 108, 34 114

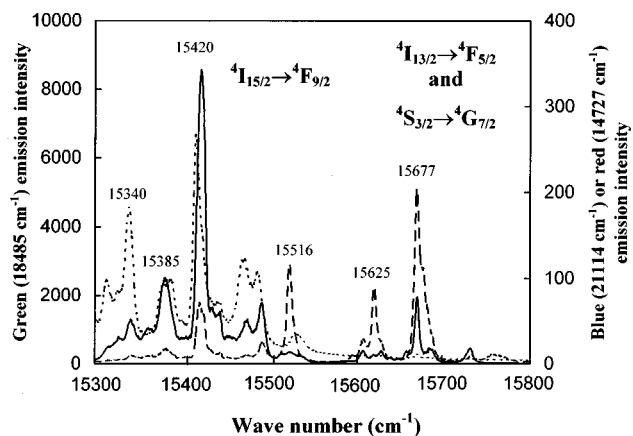


FIG. 3. Excitation spectra (recorded at 300 K) for the green, blue, and red emissions of CAGG:1% Er^{3+} . The experimental conditions are the same as those for Fig. 2.

With the similar intensity to those for the ${}^4I_{15/2} \rightarrow {}^4F_{9/2}$ transition, these lines can be assigned to the ${}^4I_{13/2} \rightarrow {}^4F_{5/2}$ transition. With regard to the blue emission, the excitation spectrum appears only in the second region, and the GSA spectrum almost disappears completely. Furthermore, this spectrum is also different from the excitation spectrum of the ${}^4I_{13/2} \rightarrow {}^4F_{5/2}$, and therefore, is probably owing to another transition: ${}^4S_{3/2} \rightarrow {}^4G_{7/2}$.¹⁴ The local surrounding effect in CAGG on the energy levels of Er^{3+} is such that both ESA (${}^4I_{13/2} \rightarrow {}^4F_{5/2}$ and ${}^4S_{3/2} \rightarrow {}^4G_{7/2}$) perfectly overlap between 15 500 and 15 800 cm^{-1} , whereas the GSA ${}^4I_{15/2} \rightarrow {}^4F_{9/2}$ is located on the low energy side.

Two optimal excitation lines (15 423 and 15 677 cm^{-1}) were selected, both inducing a strong green emission with comparable intensities. The red emission is three times (under 15 423 cm^{-1}) and 20 times (under 15 677 cm^{-1}) weaker than the green one. The blue emission only grows appreciable under 15 677 cm^{-1} . Part of the energy levels involved in the upconversion have been obtained by analyzing the emission and excitation spectra. The result is given in Table I.

At room temperature, the green upconversion intensity is reduced to about half of that observed at low temperature, while the blue upconversion shows a much weaker intensity. The excitation spectrum for the red emission is similar to that observed at low temperature. For the green and blue upconversions, however, the relative intensity for the GSA and ESA changes significantly. The GSA ${}^4I_{15/2} \rightarrow {}^4F_{9/2}$ transition is greatly enhanced. The ratio of the excitation intensities for the 15 423 (15 420) and 15 677 cm^{-1} excitation lines change from 1:0.7 to 1:0.25 for monitoring green emission and from 1:15 to 1:3 for monitoring the blue emission. This phenomenon can be explained by the energy transfer between Er^{3+} ions. At low temperature, the energy transfer is not very efficient; with increasing temperature, the nonradiative energy transfer between Er^{3+} ions becomes more efficient, resulting in the increase of the ${}^4I_{15/2} \rightarrow {}^4F_{9/2}$ transition probability. The room temperature excitation spectra for the three emissions are shown in Fig. 3.

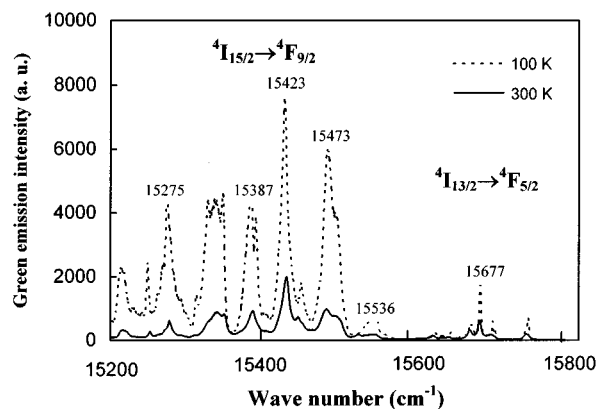


FIG. 4. Excitation spectra for the green upconversion of the Er^{3+} ion in CAGG:5% Er^{3+} at 100 K: (a) monitoring 18 490 cm^{-1} and 300 K (b) monitoring 18 485 cm^{-1} .

In order to find the optimal concentration for Er^{3+} , we have synthesized a series of samples with different Er^{3+} concentrations ranging from 0.5 to 10 mol %. The emission spectra obtained for different concentrations show the same profile, implying only one principal crystallographic site, the eightfold Ca^{2+} , in this case. The octahedral Al^{3+} site is seldom occupied by the rare earth ions due to the great mismatch in the ionic radii.¹⁵

At low temperature, the concentration effect was evaluated by measuring the relative emission intensities of the green and blue upconversions with different excitations. The optimal concentrations for green and blue emissions are both 5%. For higher Er^{3+} concentrations, the relative intensity for the GSA excitation increases and that for the ESA transition decreases compared to the lower concentration samples, as shown in Fig. 4 for monitoring the green emission from the 5% sample at 100 and 300 K. Similar results have been detected for monitoring the blue emission.

These results can also be explained by the energy transfer effect between the Er^{3+} ions. At high concentration, the average distance between the Er^{3+} ions is short, and more excited Er^{3+} ions can be found within the effective energy transfer distance. Therefore, the energy transfer efficiency is relatively high to increase the GSA excitation intensity. At higher concentration, emission intensities decrease due to the concentration quenching effect.

Upon cw laser excitation, the dynamic properties for upconversion fluorescence were analyzed at two excitation wave numbers, 15 423 and 15 677 cm^{-1} . The buildup time of the green upconversion is much different depending on whether the excitation is resonant with the GSA and ESA transitions (Fig. 5). Time constants of 1 and 5 ms were observed for 15 423 and 15 677 cm^{-1} excitations, respectively. The fluorescence decay curve for green upconversion is exponential with a time constant of 45 μs for the 15 677 cm^{-1} excitation, whereas that for the 15 423 cm^{-1} excitation consists of two exponential components with time constants of 40 and 300 μs . These decay characteristics indicate an energy transfer process being responsible for populating the ${}^4S_{3/2}$ level because the lifetimes for the upper lying levels are much shorter than 300 μs (for example, less than 10 μs for

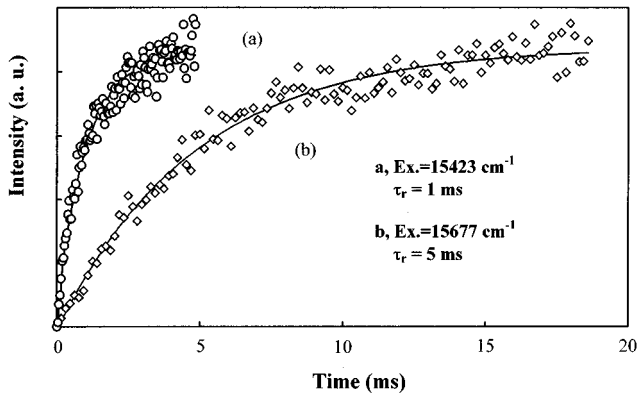


FIG. 5. Fluorescence rise curves for the green upconversion at $18\,490\text{ cm}^{-1}$ with excitation into the GSA (a) and ESA (b) transitions.

the ${}^2H_{11/2}$ manifold). For blue emission, the rise and decay constants are 4 ms and $65\ \mu\text{s}$, under $15\,677\text{ cm}^{-1}$ excitation, respectively.

The dependence of the green and blue upconversions as a function of the incident laser power are depicted in Fig. 6. The green emission intensity varies as I^2 (I being the excitation power) and the blue one as I^3 (Fig. 6). The filling mechanism of the ${}^2P_{3/2}$ level consists of three successive absorptions exciting the Er^{3+} ion from ${}^4I_{15/2}$ to a vibronic sideband of ${}^4F_{9/2}$, from ${}^4I_{13/2}$ to ${}^4F_{5/2}$, and from ${}^4S_{3/2}$ to ${}^4G_{7/2}$.¹⁴ After each absorption, the Er^{3+} ion relaxes to a metastable level which is the starting point of the next transition. Under $15\,677\text{ cm}^{-1}$ excitation, ESA (${}^4I_{13/2} \rightarrow {}^4F_{5/2}$) contributes to the ${}^4S_{3/2}$ population, whereas an energy transfer between two Er^{3+} ions excited in the ${}^4I_{11/2}$ state happens under $15\,423\text{ cm}^{-1}$. Note that at high Er^{3+} concentration, the GSA peaks are reinforced compared to the ESA ones for monitoring the blue upconversion, indicating that the nonradiative energy transfer efficiency is enhanced with increasing the Er^{3+} concentration. Therefore, the avalanche process does not happen in this system, because this mechanism operates more efficiently at high concentration. The proposed upconversion mechanisms are shown in Fig. 7.

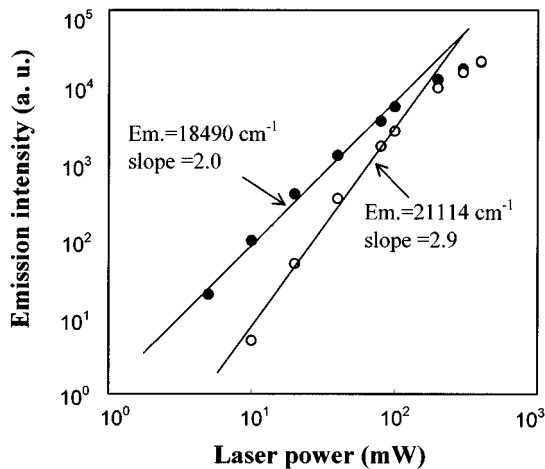
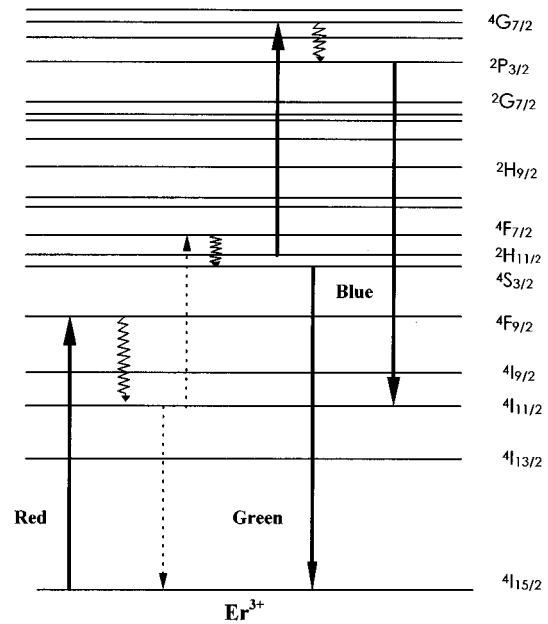
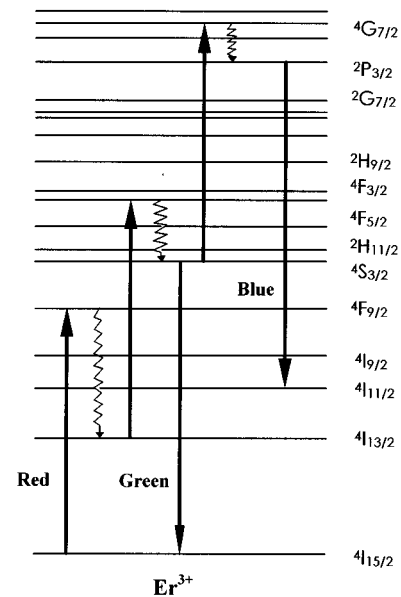


FIG. 6. Dependence (at 100 K) of the green and blue emission intensities of CAGG:1% Er^{3+} on the laser power excited with $15\,677\text{ cm}^{-1}$.



(a) Energy transfer



(b) Sequential three-step absorption

FIG. 7. Energy level diagrams of the energy transfer (a) and sequential three-step absorption (b) mechanisms for Er^{3+} in CAGG.

IV. CONCLUSION

The upconversion fluorescence of Er^{3+} in CAGG polycrystal material has been detected in several spectral ranges resulting from three energy levels: ${}^4S_{3/2}$, ${}^2H_{11/2}$, and ${}^2P_{3/2}$, upon red laser excitation at 100 and 300 K. The green emission corresponding to the ${}^4S_{3/2}$ transition appears as the most intense upconversion, which is even more intense than the red emission. The filling mechanism for the ${}^4S_{3/2}$ level is either an energy transfer involving two Er^{3+} ions excited in ${}^4I_{11/2}$ multiplet or an excited state absorption raising from the ${}^4I_{13/2}$ multiplet with regard to the laser excitation being tuned on GSA or ESA transitions, respectively. The blue emission

results mainly from a three-step absorption process with the $^4I_{13/2}$ and $^4S_{3/2}$ as the metastable levels. The effect of the temperature and the concentration on the upconversion fluorescence is such that the GSA is reinforced compared to the ESA with increasing the temperature or the Er^{3+} concentration, thus indicating that the avalanche effect is not operating in this system.

We have also demonstrated that the red-to-green upconversion of Er^{3+} is very efficient in this material, even at room temperature. The emission intensity is comparable with that observed for Er^{3+} in fluoride systems. This result implies that the CAGG can be a promising host material for the upconversion laser along with its high chemical durability and thermal stability.

¹W. Lenth and R. M. Macfarlane, *Opt. Photonics News*, 8 (March, 1992).
²F. E. Auzel, *Proc. IEEE* **61**, 758 (1973).

³N. Bloembergen, *Phys. Rev. Lett.* **2**, 84 (1959).
⁴L. Esterowitz and J. Noonan, *Optical Properties of Ions in Crystal*, edited by H. M. Crosswhite and H. W. Moos (Wiley, New York, 1966).
⁵F. E. Auzel, *C. R. Acad. Sci.* **262B**, 1016 (1966); **263B**, 819 (1966).
⁶J. C. Chivian, W. E. Case, and D. D. Eden, *Appl. Phys. Lett.* **35**, 124 (1979).
⁷P. P. Feofilov and V. V. Ovsyankin, *Appl. Opt.* **6**, 1828 (1967).
⁸N. Pelletier-Allard and R. Pelletier, *Phys. Rev. B* **36**, 4425 (1987).
⁹T. J. Whitley, C. A. Millar, R. Wyatt, M. C. Brierley, and D. Szbesta, *Electron. Lett.* **27**, 1785 (1991).
¹⁰S. Tanabe, K. Suzuki, N. Soga, and T. Hanada, *J. Lumin.* **65**, 247 (1995).
¹¹M. Malinowski, Z. Frukacz, M. F. Joubert, B. Jacquier, and C. Linares, *Appl. Phys. B* **62**, 149 (1996).
¹²L. H. Spangler, B. Farris, E. D. Filer, and N. P. Barnes, *J. Appl. Phys.* **79**, 573 (1996).
¹³X. Zhang, J. P. Jouart, G. Mary, X. Liu, and J. Yuan, *J. Lumin.* (in press).
¹⁴J. P. Jouart, M. Bouffard, X. Zhang, and G. Mary, *Ann. Phys. (Paris)* **20**, 119 (1995).
¹⁵Ph. Avouris, I. F. Chang, P. H. Duvigneaud, E. A. Giess, and T. N. Morgan, *J. Lumin.* **26**, 213 (1982).